Gene 591 (2016) 191–200

Contents lists available at ScienceDirect

Gene

journal homepage: www.elsevier.com/locate/gene

Research paper

Target genes of Dpp/BMP signaling pathway revealed by transcriptome profiling in the early *D. melanogaster* embryo

Calixto Dominguez [a,1], Alejandro Zuñiga [a], Patricia Hanna [a,b], Christian Hodar [a,b], Mauricio Gonzalez [a,b], Verónica Cambiazo [a,b,*]

[a] Laboratorio de Bioinformática y Expresión Génica, INTA-Universidad de Chile, El Libano 5524, Santiago, Chile
[b] Fondap Center for Genome Regulation (CGR), Chile

ARTICLE INFO

Article history:
Received 10 March 2016
Received in revised form 5 July 2016
Accepted 5 July 2016
Available online 7 July 2016

Keywords:
Drosophila
Dpp signaling
Dorsal ectoderm patterning
Amnioserosa
CG13653
Microarray

ABSTRACT

In the early *Drosophila melanogaster* embryo, the gene regulatory network controlled by Dpp signaling is involved in the subdivision of dorsal ectoderm into the presumptive dorsal epidermis and amnioserosa. In this work, we aimed to identify new Dpp downstream targets involved in dorsal ectoderm patterning. We used oligonucleotide *D. melanogaster* microarrays to identify the set of genes that are differential expressed between wild type embryos and embryos that overexpress Dpp (*nos*-Gal4>UAS-*dpp*) during early stages of embryo development. By using this approach, we identified 358 genes whose relative abundance significantly increased in response to Dpp overexpression. Among them, we found the entire set of known Dpp target genes that function in dorsal ectoderm patterning (*zen*, *doc*, *hnt*, *pnr*, *ush*, *tup*, and others) in addition to several up-regulated genes of unknown functions. Spatial expression pattern of up-regulated genes in response to Dpp overexpression as well as their opposing transcriptional responses to Dpp loss- and gain-of-function indicated that they are new candidate target genes of Dpp signaling pathway. We further analyse one of the candidate genes, CG13653, which is expressed at the dorsal-most cells of the embryo during a restricted period of time. CG13653 orthologs were not detected in basal lineages of Dipterans, which unlike *D. melanogaster* develop two extra-embryonic membranes, amnion and serosa. We characterized the enhancer region of CG13653 and revealed that CG13653 is directly regulated by Dpp signaling pathway.

1. Introduction

It is now well established that the graded concentration of a signaling molecule, known as morphogen, organizes and patterns tissues in developing animals (Wolpert, 1996). Studies in *Drosophila melanogaster* and in vertebrates have revealed that extracellular activity gradients of morphogens, such as members of the Hedgehog, Wingless and TGFβ families of signaling molecules, regulate the expression of target genes in a concentration-dependent manner (Raftery and Sutherland, 2003). In the early *D. melanogaster* embryo, the combined actions of two morphogens, Decapentaplegic (Dpp), the *Drosophila* functional ortholog of mammalian BMP2/4, and Screw (Scw) control the subdivision of dorsal ectoderm into presumptive dorsal epidermis and amnioserosa, an extraembryonic membrane that develops at the dorsal-most region of the embryo. The amnioserosa is found in higher cyclorrhaphan flies, such as *D. melanogaster* however in other dipterans, dorsal ectoderm patterning gives rise to distinct serosal and amniotic epithelia (Rafiqi et al., 2008; Schmidt-Ott et al., 2010).

During dorsal ectoderm patterning, Dpp and Scw form an extracellular gradient with peak levels of signaling at the dorsal-most region of the embryo (Raftery and Sutherland, 2003). The shaping of the Dpp gradient from an initially uniformly distributed mRNA is achieved by the combined action of extracellular Dpp binding proteins and metalloproteases (Matsuda et al., 2016). In the early embryo, Dpp acts as an inductive morphogen; however Scw enhances the pathway activity along the dorsal midline and is required for amnioserosa specification (Arora et al., 1994). Dpp/Scw signal trough Type I and Type II receptors leading to the phosphorylation of the Smad transcription factor, Mothers-against-dpp (Mad). Phosphorylated Mad (pMad) forms a complex with a co-Smad, known as Medea (Med), and both translocate into the nucleus to activate transcription of an undetermined number of target genes (Parker et al., 2004). Within the regulatory regions of known target genes, Mad/Medea bind to sites containing repeats of the degenerate sequence GNCN, which is consistent with the sequence of the Smad

Abbreviations: DIG, digoxigenin; FITC, fluorescein isothiocyanate; DAPI, 4′,6-diamino-2-fenilindol; PBS, phosphate-buffered saline; Cy3, cyanine 3; Cy5, cyanine 5; PCR, polymerase chain reaction.

* Corresponding author at: Laboratorio de Bioinformática y Expresión Génica, INTA-Universidad de Chile, El Libano 5524, Santiago, Chile.
E-mail address: vcambiaz@inta.uchile.cl (V. Cambiazo).
[1] Current address: Computational Biology Lab, Center for Bioinformatics and Genome Biology, Fundacion Ciencia y Vida. Zañartu 1482, Santiago, Chile.

http://dx.doi.org/10.1016/j.gene.2016.07.015
0378-1119/

binding element (SBE) GTCT found in the response regions of TGFβ target genes (ten Dijke et al., 2000).

Most of the known targets of Dpp/Scw signaling are required for amnioserosa development. For example, *zen*, a homeotic gene that is responsible of all aspects of amnioserosa differentiation (Rushlow and Arora, 1990) and the *u-shaped* group of genes that encode transcription factors involved in the maintenance of amnioserosa once it has been differentiated (Frank and Rushlow, 1996; Yip et al., 1997; Reim et al., 2003). Recently, it has been shown that proper formation of Dpp gradient in the early embryo depends on a feedback regulation provided by the products of two target genes of Dpp pathway, *eiger* and *crossvein-2*, which stimulate and antagonize Dpp signaling, respectively (Wang et al., 2008; Gavin-Smyth et al., 2013).

In a previous work, we identified *Dtg*, a new target gene of Dpp signaling, which encodes a novel secreted protein with roles in amnioserosa maintenance (Zúñiga et al., 2009; Hodar et al., 2014). Here, we aimed to identify new Dpp downstream targets involved in dorsal ectoderm patterning. To do this, we used microarray transcriptome profiling, which enabled us to find direct and indirect transcriptional targets, including those which are difficult to identify in traditional mutant screens due to pleiotropy and/or functional redundancy. In addition, we further characterize gene CG13653 whose expression at the dorsal-most region of the early embryo was directly controlled by Dpp signaling.

2. Methods

2.1. Fly culture and embryo selection

Adults were grown at 22 °C on standard cornmeal, molasses, agar and yeast medium. Embryos were collected as described in Zúñiga et al. (2009). Flies carrying UAS-*dpp* have been described (FlyBase ID: FBst0001486), they were crossed to a Gal4 driver in which the Gal4 protein is expressed under the control of the enhancer of the maternal gene *nanos* (FlyBase ID: FBst0004442). In these embryos, induction of ectopic Dpp results in a broader longitudinal stripe of nuclear pMad when compared with wild type embryos (Hodar et al., 2014). In control embryos expression of *lacZ* was driven by *nanos*-Gal4 (*nos*-Gal4>*lacZ*). The alleles of mutant genotypes were: dpp^{hr92} a hypomorphic *dpp* allele balanced over *Cyo*, *ftz-lacB* (Wharton et al., 1993), dpp^{H46} a null *dpp* allele balanced over *CyO23*, P[*dpp* +] (Wharton et al., 1993), sog^{s6} balanced over FM7, *ftz-lacZ* (Hamaguchi et al., 2004) and brk^{M68} balanced over FM7, *ftz-lacZ* (Weiss et al., 2010). Homozygous mutant embryos were distinguished by the lack of *lacZ* mRNA detection in double *in situ* hybridizations. To obtain staged embryos, females were allowed to lay eggs for 2 h on 2% apple juice agar plates spread with live brewer's yeast. The plates were replaced several times and finally one-hour embryos were collected, dechorionated and washed with Ringer *Drosophila* solution (182 mM KCl, 46 mM NaCl, 3 mM CaCl2, 10 mM Tris-HCl, pH 7,2). Embryos were selected at stages 2–3 (syncytial blastoderm) or 5 (cellular blastoderm) and then allowed to continue their development in a humidified chamber at 25 °C. We hand-selected embryos at late stage 5 to stage 7 based on their morphological characters (Campos-Ortega and Hartenstein, 1985), and rapidly frozen them in liquid N_2. Embryos were kept at −80 °C for 1–2 weeks.

2.2. In situ hybridization of whole-mount embryos

In situ hybridizations using 1–2 ng/μL DIG-labelled RNA probes were carried out essentially as described in Hodar et al. (2014). A plasmid bearing a *lacZ* insert (gift of Dr. M. Levine) was employed to prepare a RNA probe to detect the expression of the *lacZ* transgene. Double *in situ* hybridizations of *D. melanogaster* embryos were performed using FITC- and DIG-labelled RNA probes, a sheep anti-DIG primary antibody (Roche) and a mouse anti-FITC primary antibody (Roche). Embryos were mounted in 80% glycerol and photographed under differential interference contrast (DIC) optics.

2.3. Immunohistochemistry of embryos

Embryos were fixed and treated as described in Zúñiga et al. (2009). Primary antibody was polyclonal anti-phospho-Smad (phospho S423 + S425, Abcam, 1:50) and secondary antibody was anti-rabbit Alexa 488 (Jackson, 1:500). Nuclear staining was made with ToPro (Molecular Probes, 1:200). Fluorescently-labelled embryos were mounted in DAKO or in 3:1 Glycerol:PBS. Confocal images were collected using confocal microscope C2+ (Nikon) and processed using NIS-Elements Microscope Imaging Software (Nikon) and Image J (NIH).

2.4. RNA extraction and preparation of spike mRNAs

Total RNA from *nos*-Gal4>*lacZ*, *nos*-Gal4>UAS-*dpp* embryos (N = 100–200) at late stage 5 (cellularization) to early stage 7 (gastrulation) of development was extracted as described in Zúñiga et al. (2009). RNA was quantified using Qubit RNA HS Assay Kit (Thermo Fisher) and the integrity was assayed in Tape station 2200 (Agilent Technologies). For microarray experiments, 50 pg of spike mRNAs was added to each RNA preparation prior to labelling. The three spike genes were *Bacillus subtilis* tryptophan operon, *trpCDEF* (ATCC 87485), diaminopimelate decarboxylase gene *lysA* (ATCC 87482) and dihydrodipicolinate reductase gene, *dapB*, (*ATCC 87486*). Each vector consists of bacterial cDNA cloned into the *Xho*I and *Bam*HI sites of a modified pBluescript II-KS+ vector in which a poly(dA) stretch follows the *Bam*HI restriction site. From each vector, RNA transcripts containing a poly(A) tract were generated using the Riboprobe Combination System (Promega). Predicted transcript sizes were confirmed using denaturant agarose gel electrophoresis.

2.5. Probe synthesis and microarray hybridization

To prepare the fluorescent probes, total RNA was amplified using the Amino Allyl MessageAmp II aRNA Amplification Kit (Ambion, Texas) following the manufacturer's instructions. Labelled aRNA was purified using QIAquick columns (Qiagen), yield and specific activity of each probe was determined by absorption spectroscopy. Pairs of Cy3 and Cy5 labelled aRNA probes (2.5 μg/probe) were pooled, fragmented (Ambion RNA Fragmentation Reagent) and hybridized to the *D. melanogaster* microarrays. The experimental samples were tagged with Cy5 and the control samples with Cy3. In separate hybridizations, the labelling of the samples was dye-swapped.

Oligonucleotide *D. melanogaster* microarrays were purchased from Microarray Inc. and contained 14,593 probes designed from the Gadfly release 3.1 database, they represent 13,664 genes and 17,899 transcripts. Oligonucleotides corresponding to genes coding for the spikes RNAs were randomly distributed in different blocks throughout the array. Microarrays were pre-washed in 50 mL of pre-hybridization buffer (5 × SSC, 0.1% SDS, 0.1% BSA Fraction V) for 60 min at 42 °C, then 5 times in ddH_2O for 1 min at room temperature. After the pre-washing, microarrays were dried by centrifugation. Then, microarrays were hybridized with labelled probes in a hybridization solution containing 20% formamide, 5× SSC and 0.1% SDS. Hybridized slides were sequentially washed 4 times by 15 min in 2× SSC, 0.1% SDS, 4 times by 5 min in 0.1× SSC, 0.1% SDS and then rinsed 4 times by 1 min in 0.1× SSC.

2.6. Microarray experimental design and data analysis

Two independent control (*nos*-Gal4>*lacZ*) and experimental (*nos*-Gal4>UAS-*dpp*) samples (biological replicates) were hybridized onto nine slides, and dye-swap replicates were conducted in the first hybridization. Images were processed using the software ScanArray Express (Perkin Elmer) to align both channels at different PTM gain. Image quality was assessed by *q.com* descriptors included within the R function, (Wang et al., 2001). Additionally, control spots (spike controls, empty spots and random oligomers) were analysed separately to distinguished high quality hybridized slides. Data from slides were processed to

remove noise using normexp (Ritchie et al., 2007), normalized by block with *loess* (Smyth and Speed, 2003) and differentially expressed genes were identified using the statistical R package LIMMA (Smyth, 2004). LIMMA is able to estimate the coefficients of the contrast matrix between the conditions and fits a linear model for each gene. Estimation of significance is based on a hypothesis test that uses the statistical *t*-moderate associated to *p*-value. In addition, a Bayesian statistical analysis was included which is based on the calculation of the posterior probability estimated from prior probability conditionality. *p*-Values were adjusted by the method of Benjamini and Hochberg (1995) to control the rate of false values. Genes with statistically significant changes in expression (adjusted *p*-value <0.05) were selected. Gene Ontology (GO), protein domain enrichment and ImaGO terms enrichment were carried out for each gene within the FlyMine portal using the *Drosophila* genome as background dataset and Holm-Bonferroni multiple testing correction. For enrichment, FlyMine uses a hypergeometric distribution, and the Holm-Bonferroni correction was applied to get the adjusted *p*-values. Microarray data were submitted to Gene Expression Omnibus (GEO, accession number: GSE78226).

2.7. Genotyping of dpp^{hr92} homozygous embryos and RNA extraction

Homozygous embryos were selected using a genotyping procedure described by Ghanim and White (2006). In our case, both the absence of *lacZ* specific band together with the presence of a control band (non-coding region of gene *Dtg*) were indicators of homozygous lethal embryos.

For RNA extractions, extracts of homozygous (dpp^{hr92}) and heterozygous (dpp^{hr92}/*Cyo*, *ftz-lacB*) staged embryos previously preserved in RNA_{WIZ} reagent (N = 50) were pooled, then samples were carefully homogenized in a 1.5 mL Eppendorf tube on ice with the aid of RNAse-free polypropylene pellet pestle. After homogenization, RNA extraction was performed using standard protocols. RNA was quantified using Qubit® RNA HS Assay Kit (Thermo Fisher) and the integrity was assayed in Tape station 2200 (Agilent Technologies). Samples were treated with Turbo DNA-free DNase (Ambion) to remove contaminating DNA.

2.8. cDNA synthesis and quantitative real-time quantitative PCR (qPCR) assays

The high capacity RNA to cDNA kit (Applied Biosystems) was used to synthesize cDNA from *nos*-Gal4>*lacZ* and *nos*-Gal4>UAS-*dpp* embryo aRNAs and total RNA from dpp^{hr92} and dpp^{hr92}/*Cyo*, *ftz-lacB* (dpp^{hr92}/+) embryos. All reactions were carried out according to manufacturer instructions and one μg of the embryo RNA was used as template. For qPCR assays, reactions were carried out on an Mx3005P Stratagene (Agilent) using LightCycler FastStart DNA Master SYBR Green kit (Roche Applied Science). PCR conditions were 95 °C for 5 min followed by 94 °C for 15 s, 57–60 °C for 15 s and 72 °C for 20 s for a total of 35 cycles. Melting curves (1 °C steps between 75 and 95 °C) ensured that a single product was amplified in each reaction. To determine relative expression levels of genes, the method described by Pfaffl (2001), and adapted by Talke et al. (2006) was used and *tbp* was employed as internal reference gene. Three independent biological replicates of each condition tested were used to performed the qPCR assays, and for each biological replicate at least two technical replicates of each PCR reaction were run. Differences among conditions were analysed using Student's *t*-test ($p < 0.05$). A complete list of primers is in Supplementary Table S1.

2.9. De novo Mad-binding sites prediction

The non-coding regions (introns, untranslated-5′ and −3′ and 2 kb upstream from the transcriptional start site) of genes up-regulated in *nos*-Gal4>UAS-*dpp* embryos were scanned using Patser (Hertz and Stormo, 1999) with a consensus matrix built from 26 experimentally validated Mad binding sites. These Mad-binding sites are contained within functional enhancers of ten Mad target genes *Ubx-B* (Thuringer et al., 1993), *Ance* (Wharton et al., 2004), *C15* (Lin et al., 2006), *bam* (Chen and McKearin, 2003), *tin* (Xu et al., 1998), *vg* (Kim et al., 1997), *zen* (Rushlow et al., 2001), *lab* (Kim et al., 1997), *pnr* (Liang et al., 2012), *Dtg* (Hodar et al., 2014). Predicted motifs that were statistically significant (*p*-value ≤0.05) were clustered within a window of 50 bp length. A cluster was composed by a minimum of two Mad motifs with at least one base pair of overlapping. Then, the enhancer database annotated with ontological controlled vocabulary (http://enhancers.starklab.org) (Kvon et al., 2014) was queried to identify the genome regions that harbored predicted clusters of Mad-binding sites within fragments that drive *in vivo* reporter gene expression in the dorsal ectoderm. Coding and non-coding regions of CG13653 orthologs from twelve *Drosophila* species were aligned using MLAGAN (Brudno et al., 2003) algorithm and the alignments were visualized using the VISTA Genome Browser (Frazer et al., 2004), conservation was measured using an 80 bp window and a cut-off score of 50% of identity in a row of 60 bp.

2.10. Construction of reporter plasmid, site-directed mutagenesis and transgenesis

Genomic *D. melanogaster* DNA was prepared as described in Bellen et al. (2004) with minor modifications: homogenized samples were incubated at 70 °C and precipitated in ice for 30 min in presence of KOAc solution (5 M, pH 5.2). A phenol/chloroform extraction followed by ethanol precipitation was used in order to purify the DNA. Sequences of DNA fragments were extracted from FlyBase R5/dm3 (Attrill et al., 2015). DNA fragments encompassing nucleotides +27 to −781, −389 to −781 and +27 to −375 relative to the CG13653 transcriptional start site were amplified by PCR. The forward primer sequences were as follows: 5′-CGACAGTGGCAATGGCTTAC-3′ (map positions −781 to −761); 5′-GACTGAGGACTGGACGCG-3′ (−375 to −357). Reverse primers were: 5′-ATCGATGTGCTTCGTTCGGT-3′ (+8 to +27) and 5′-CACAGGACCAAG CTGGACG-3′ (−408 to −389). PCR products were purified, cloned into the pGEMT-Easy vector (Promega) and sequenced. Fragments were subcloned into the gypsy-insulated pPelican vector (Barolo et al., 2000). Site directed mutagenesis was performed by GenScript (Piscataway, NJ). Constructs were sent to BestGene Inc. for production of transgenic flies. For each transgene, three independent insertions were analysed.

2.11. Identification of CG13653 orthologs and protein alignments

Orthologs for *D. melanogaster* CG13653 predicted protein were searched in OrthoDB database (Waterhouse et al., 2011) and the sequences of CG13653 orthologs were collected from FlyBase database. Progressive alignment of the twelve *Drosophila* protein sequences (FlyBase) were performed using MUSCLE software (Edgar, 2004) with 100 iterations and two steps for clustering: neighbour joining and UPGMA. Search for ortholog proteins in *Anopheles gambiae* (Ensembl, release 3.22) *Aedes aegypti* (Vectorbase, release 3.22) and *Musca domestica* (NCBI: GCF_000371365.1) genomes were performed using blastp alignments against available databases and the following including criteria: E-value = 1×10^{-5}, a minimum of 30% of identity and alignment coverage >50%.

3. Results and discussion

3.1. Identification of Dpp responsive genes by microarray analysis

To identify candidate Dpp target genes, we performed a microarray analysis using a *Drosophila* array that contains probe sets interrogating 13,664 genes. The *nos*-GAL4 maternal driver was used to express *dpp* or *lacZ* in early embryos, and RNA was collected from carefully selected embryos at late stage 5 (cellularization) to early stage 7 (gastrulation). As a first step, we verified the downstream effects of Dpp overexpression by

immunofluorescence assays to detect the expression pattern of the phosphorylated, and hence activated, form of Mad (pMad) in *nos*-Gal4>UAS-*lacZ* (control) and *nos*-Gal4>UAS-*dpp* (Fig. 1). In control embryos high levels of pMad were detected along a stripe of five to six dorsal cells, whereas cells at either side of the stripe showed low or undetectable levels of the protein. This is the reported expression pattern of pMad since at early stages of development a sharp gradient of pMad is formed in dorsal cells as a consequence of the peak levels of Dpp activity (Dorfman and Shilo, 2001). In *nos*-Gal4>UAS-*dpp* embryos, which overexpress Dpp, we observed a significant widening of the dorsal-longitudinal stripe of pMad expression (Fig. 1A), which was accompanied by a significant increase in the relative expression levels of four well-known target genes of Dpp signaling pathway (Fig. 1B).

For the microarray experiment, total RNA from staged *nos*-Gal4>UAS-*lacZ* (control) and *nos*-Gal4>UAS-*dpp* embryos was prepared and hybridized in biological duplicates to the *Drosophila* array, and candidate Dpp target genes were identified by comparing gene-expression profiles of embryos overexpressing *dpp* to embryos expressing *lacZ*. This comparison yielded 640 transcripts whose relative abundance increases (56%) or decreases (44%) significantly in response to higher Dpp level (GEO, accession number: GSE78226).

Among the significantly up-regulated genes (Supplementary Table S2), we identified a number of genes previously shown to be induced by Dpp signaling, including genes with roles in dorsal ectoderm patterning and amnioserosa maintenance, *zen*, *dad*, *doc 1*, *doc 2*, *doc 3*, *hnt*, *pnr*, *ush*, *tup* (Frank and Rushlow, 1996; Rushlow et al., 2001; Reim et al., 2003) and genes implicated in the formation of the Dpp/Scw gradient such as, *cv-2* and *egr* (Wang et al., 2008; Gavin-Smyth et al., 2013), which are transcriptionally regulated by pMad and the Dpp target gen, *zen*. Additional known Dpp target genes that were induced in *nos*-Gal4>UAS-*dpp* embryos included: *so* and *eya*, which are required for optic lobe fate (Chang et al., 2001), *dap*, which encodes a specific inhibitor of Cyclin E/Cdk2 complexes (Liu et al., 2002), *kay* encoding an homologue of the mammalian proto-oncogene product, c-Fos (Dequier et al., 2001), *chrb*, a putative regulator of apoptosis with roles in head involution, a morphogenetic process that is partially controlled by Dpp signaling (Scuderi et al., 2006), *Follistatin* and *Ect4* (Saunders et al., 2013). For some of the up-regulated genes Mad-responding enhancers have been characterized, for instance, *Ance*, *C15*, *zen*, *pnr*, *dad* and *Dtg* (Rushlow et al., 2001; Xu et al., 2005; Lin et al., 2006; Weiss et al., 2010; Liang et al., 2012; Hodar et al., 2014). In addition to this set of known Dpp target genes, our experimental approach was able to recover other known genes not yet associated to dorsal-ventral patterning (for instance: *Wnt4*, *Sema5c*, *dlp*) and several novel genes of unknown functions denoted by the prefix CG (Supplementary Table S2).

Then, we addressed whether the up-regulated genes were enriched for genes of any functional classes. When Gene Ontology enrichment analysis was conducted with the Flymine service (v. 42.1) (Lyne et al., 2007) significant over representation of a number of related gene categories was observed (Supplementary Table S3). Among terms describing biological processes, there was enrichment for genes annotated for roles in tissue, organ and development of embryo structures, for example we found the GO terms "pattern specification process, "eye development" and "dorsal closure" that are particularly relevant to the known regulatory functions of Dpp (Chang et al., 2001; Reim et al., 2003). With respect to molecular function there was enrichment for genes described by the terms "protein binding" and "transcription factor binding", which are consistent with the statistically significant enrichment for genes that carried a Homeobox conserved site [IPR017970].

We also addressed the question of whether the genes up-regulated in *nos*-Gal4>UAS-*dpp* embryos were expressed preferentially in the tissues in which Dpp is known to exert its functions. In doing so, we used FlyMine and the BDGB *in situ* database (Tomancak et al., 2002, 2007; Hammonds et al., 2013) to assign anatomical terms to the up-regulated genes (Supplementary Tables S2 and S3). The BDGP *in situ* database contains images of patterns of gene expression during embryogenesis for 7917 *Drosophila* genes. All expression patterns are annotated using controlled vocabulary (ImaGO terms). Even though microarrays were performed on whole embryos, the enrichment analysis revealed that many of the up-regulated genes in *nos*-Gal4>UAS-*dpp* are expressed in the dorsal region of the embryo. In particular, "dorsal ectoderm primordium" (p-value $<1.96e-24$), "amnioserosa anlage" (p-value $<7.77e-22$) and "procephalic ectoderm anlage" (p-value $<2.25e-14$) were the most statistically significant enriched anatomy terms (Supplementary Table S3). Most of the up-regulated genes expressed in the procephalic ectoderm also are expressed in the ectoderm/epidermis, the dorsal head epidermis primordium or the visual anlage/primordium. This is consistent with pMad staining in dorsal head of the embryo and in the eye field, and with the role of Dpp in partitioning the anterior brain and the eye anlage (Chang et al., 2001). Thus, enrichment analysis indicated that up-regulated genes showed a spatial distribution pattern consistent with the increased activity of Dpp signaling pathway during the development of ectodermal lineage cells. We noticed that the terms ventral ectoderm/epidermis primordia were also highly enriched in our gene list, probably due to the complex expression pattern of a group of genes, such as *betaCOP*, *nvy*, *E(spl)m7-HLH*, *tara*, *rib* and CG42342, which are detected at different domains located in dorsal and ventral structures (Supplementary Table S2), suggesting that their temporal and/or spatial regulation are under the control of separate enhancers. For some of the genes expressed in dorsal domains of the embryo we could predict clusters of Mad binding sites (Supplementary Table S2)

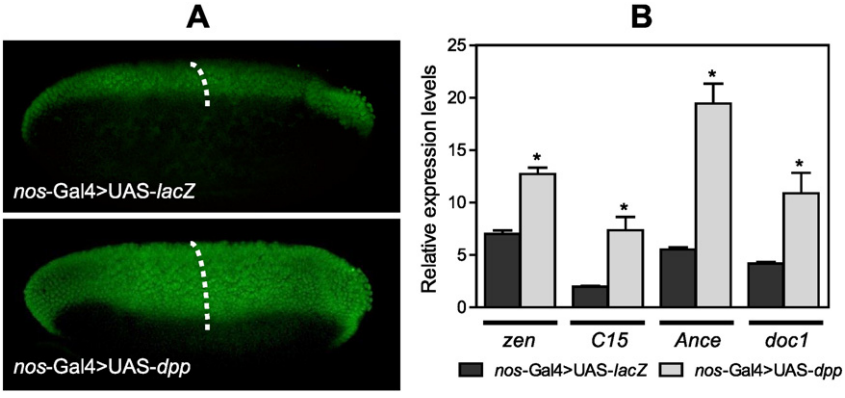

Fig. 1. Overexpression of Dpp in *nos*-Gal4>UAS-*dpp* embryos. (A) Whole-mount immunofluorescences of embryos stained with an anti-phospho-Smad antibody (green). The images correspond to lateral views of stage 6 embryos with anterior to the left. The expression pattern of pMad is restricted to a narrow strip of dorsal cells in a wild type embryo (*nos*-Gal4>UAS-*lacZ*, upper panel), whereas in an embryo that overexpress Dpp (*nos*-Gal4>UAS-*dpp*, lower panel) the expression domain of pMad is clearly wider as indicated by the segmented white line. (B) Quantitative real-time PCR shows increased expression of previously characterized Dpp target genes. Data shown are transcript levels relative to housekeeping gene *tbp*. Values correspond to the mean and SE of three independent biological replicates. Asterisks indicate significant differences among *nos*-Gal4>UAS-*lacZ* and *nos*-Gal4>UAS-*dpp* conditions that were analysed using Student's t-test ($p < 0.05$).

within a genome region with previously reported *in vivo* enhancer activity (http://enhancers.starklab.org; Kvon et al., 2014). It is noteworthy that 23 genes of unknown functions that were recovered from the screening are expressed at dorsal domains where high Dpp activity takes place in the early embryo, thus these genes constitute a good entry point for the investigation of new targets of Dpp regulation in the early embryo. In summary, our microarray studies identified a group of genes up-regulated in *nos*-Gal4>UAS-*dpp* embryos that were significantly enriched in amnioserosa and dorsal ectoderm, among them we found the entire set of genes known to be activated by Dpp at early stages of development along with several genes not previously linked to the Dpp signaling pathway.

3.2. Validation of differential expression results

Putative Dpp target genes were expected to be up-regulated upon overexpression of *dpp* and downregulated in a loss-of-function background. Therefore, we performed a quantitative real-time PCR analysis (qPCR) to verify the differential expression levels of 18 genes in dpp^{hr92} (loss-of-function) and *nos*-Gal4>UAS-*dpp* (gain-of-function) embryos compared to their respective control embryos (Fig. 2). In dpp^{hr92} mutant embryos the expression of pMad is absent as shown in Supplementary Fig. S1. For qPCR assays we selected three known Dpp target genes (*Ance*, *C15* and *Dtg*), and 15 other genes that were expressed at dorsal ectoderm and/or amnioserosa and/or procephalic ectoderm in the BDGP *in situ* database. Some of these were known genes that have not yet been associated to Dpp signaling pathway, such as *Wnt4*, *Ect4* and *Sema5c*, whereas the rest of them were genes of unknown functions and are referred to by their CG number. Except for gene CG8312, the results indicated a significantly increase in the relative expression levels of the selected genes in *nos*-Gal4>UAS-*dpp* embryos, whereas the entire set of genes decreased their expression in dpp^{hr92} embryos. These results, with the reproducibility of the individual samples analysed, establish the validity of our microarray data.

For a subset of genes of unknown functions, which were differentially up-regulated in *nos*-Gal4>UAS-*dpp* embryos, digoxygenin-labelled RNA probes were synthesized and hybridized to wild type, dpp^{hr92} and *nos*-Gal4>UAS-*dpp* embryos. In order to detect Dpp signaling activity, embryos were hybridized with a probe against gene *Dtg* (Hodar et al., 2014) (Fig. 3). With the exception of the mRNAs of gene CG12011 that was detected in the differentiated amnioserosa (Fig. 3I, as) from the stage 8 to 15 of development, and the mRNA of gene CG42342, which was mostly detected in the procephalic ectoderm (Fig. 3H, pe), the mRNAs of the other eight genes were detected in a dorsal longitudinal stripe of variable width encompassing the developing amnioserosa and dorsal ectoderm of late stage 5 to stage 7 embryos (Fig. 3B–G). Previous works have shown that the graded distribution pMad in the dorsal ectoderm results in the specification of three distinct threshold of gene expression (Ashe et al., 2000). Thus, peak levels of Dpp signaling activate the expression of genes *Ance*, *zen* and *hnt* in a stripe of 5–7 cells in the dorsal-most region of the embryo (Rusch and Levine, 1997; Ashe et al., 2000), whereas intermediate levels of Dpp signaling are required to activate the expression of *tup*, *ush* and *C15* genes in a wider stripe of 12–14 cells (Ashe et al., 2000; Lin et al., 2006). Finally, the expression of *pannier* extends to lateral regions with low to undetectable levels of pMad staining (Liang et al., 2012). We observed that the set

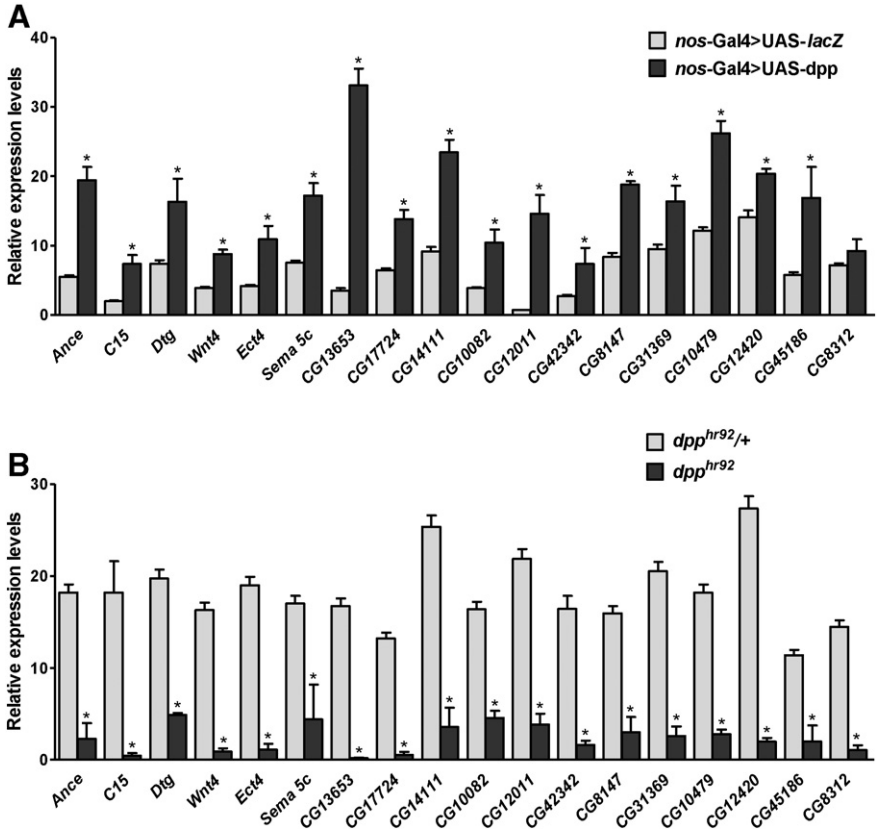

Fig. 2. Expression analysis of candidate Dpp target genes in *dpp* gain- and loss-of-function embryos. Expression changes of selected genes in dpp^{hr92} (loss-of-function) and *nos*-Gal4>UAS-*dpp* (gain-of-function) embryos were analysed by quantitative real-time PCR. Comparisons of gene expression changes were carried out between dpp^{hr92} mutant embryos and dpp^{hr92}/*Cyo*, *ftz-lacB* (dpp^{hr92}/+ in the figure) control embryos and between *nos*-Gal4>UAS-*dpp* and nos-Gal4>UAS-*lacZ* embryos. Data shown are transcript levels relative to housekeeping gene *tbp*. Values correspond to the mean and SE of three independent biological replicates and at least two technical replicates of each PCR reaction. Asterisks indicate significant differences between mutant embryos and their respective wild type controls that were analysed using Student's *t*-test ($p < 0.05$).

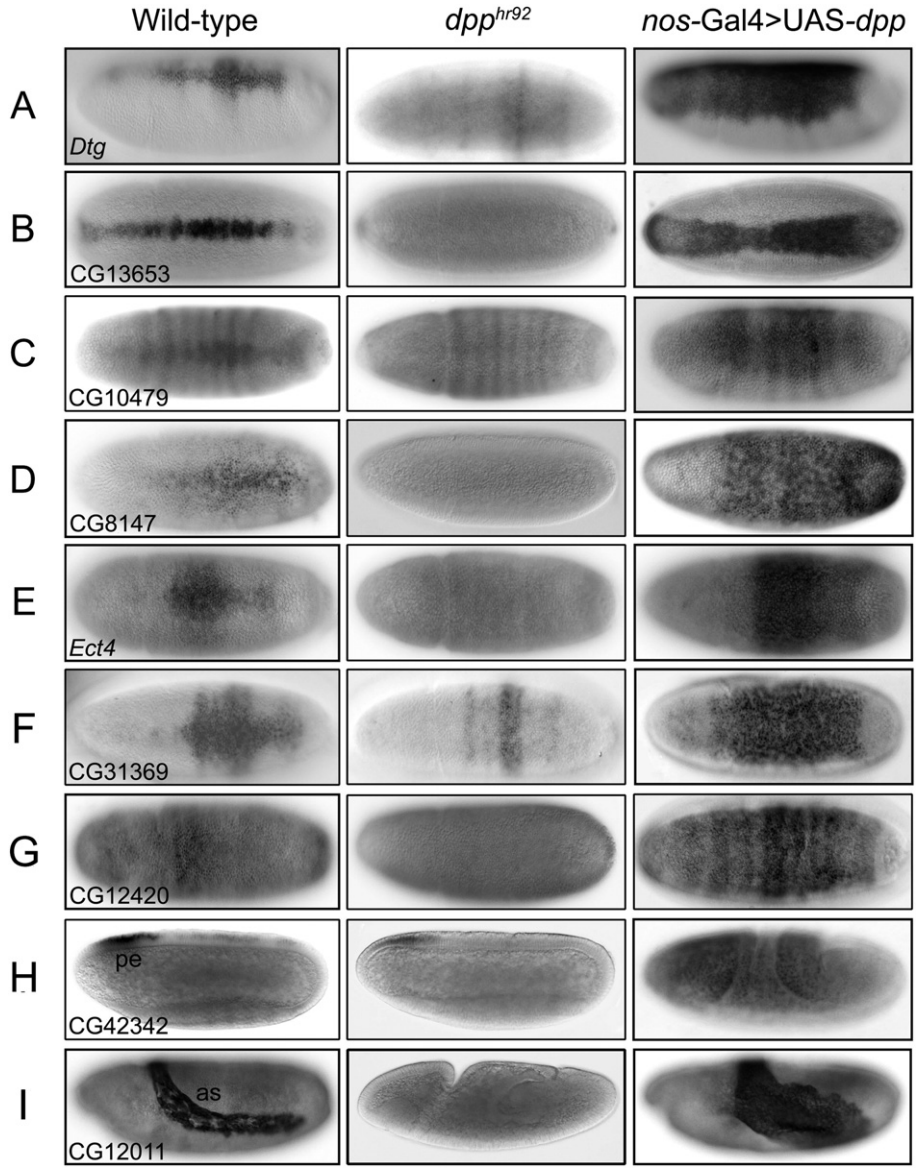

Fig. 3. Expression pattern of selected genes in wild type and mutant embryos. Whole-mount *in situ* hybridizations in wild type embryos, in dpp^{hr92} mutant embryos and in embryos that overexpress Dpp (*nos*-Gal4>UAS-*dpp*) were carried out using DIG-labelled DNA probes as described in Section 2. The expression of *Dtg*, a Dpp target gene (panels A), was used to reveal the change in Dpp signaling. In wild type embryos, *Dtg* mRNA was detected in a five- to fifteen-cell-wide dorsal strip of cells, in dpp^{hr92} embryos the longitudinal stripe of *Dtg* expression was lost, whereas in the *nos*-Gal4>UAS-*dpp* embryos a wider dorsal longitudinal stripes of *Dtg* expression was observed. Gene symbols are indicated at the bottom of the panel. Panels B to G are dorsal views of stage 6 embryos with anterior to the left. Panels H are lateral views of stages 6 and 8 embryos and panels I are lateral views of stage 9 embryos. Procephalic ectoderm (pe), amnioserosa (as).

of up-regulated genes analysed here were expressed in discrete domains along the dorsal midline and most of them exhibited different widths of expression that correlates with the previously described domains of high (CG13653, CG10479) and intermediate (CG31369, CG8147, *Ect4*) Dpp activity (Fig. 3). When the expression patterns of these genes were examined in dpp^{hr92} and in *nos*-Gal4>UAS-*dpp* embryos, we observed that the dorsal wild type expression of this set of genes was lost or severely diminished in the *dpp* mutant embryos while a wider dorsal longitudinal stripe of expression was detected in the embryos that overexpressed *dpp* (Fig. 3). In particular, the expression pattern of CG12011 revealed the enlargement of the amnioserosa in the *nos*-Gal4>UAS-*dpp* embryos (Fig. 3I). These results suggested that these genes are under the control of Dpp pathway and supported the possibility that they are target genes of Dpp signaling pathway.

Given the evidence provided here regarding the spatial expression pattern and the transcriptional behaviour of genes significantly up-regulated in response to the Dpp overexpression, it seems likely that our candidate gene list contains a group of new Dpp target genes.

3.3. CG13653 is a direct target gene of Dpp signaling pathway

One gene identified in the screen offered a particularly interesting opportunity to test whether an individual gene whose expression is up-regulated in *nos*-Gal4>UAS-*dpp* embryos is a direct target of Dpp signaling pathway. The gene CG13653 encodes a 235-amino acid predicted protein that lacks of any conserved domains, except for a potential signal peptide sequence. Using the predicted protein of CG13653, we mined the genomes of twelve *Drosophila* species as well as the available genomes from *Musca domestica*, *Anopheles gambiae*, and *Aedes aegypti*; CG13653 orthologs were only found in the Drosophilidae lineage, suggesting that CG13653 is a lineage-specific gene (Supplementary Fig. S2). Comparison of the deduced amino acid sequences of CG13653

orthologs in *Drosophila* species revealed a mean pair wise percent identity of 60.2% (Supplementary Fig. S3). Protein sequence homology between the distant sibling species *D. melanogaster* and *Drosophila grimshawi* was 50.7%. Conserved features among these sequences included a predicted signal peptide domain within the first 22 protein residues (38.6% of sequence identity).

The earliest detectable CG13653 expression was observed during embryo cellularization (stage 5) and consisted of a stripe of approximately 5–8 dorsal cells, that extends along the midline of the embryo from anterior to posterior (Fig. 4A). In early gastrula embryos (stage 6) CG13653 mRNA was detected in a dorsal longitudinal stripe of 5 to 7 cells encompassing the anlagen of the amnioserosa (Fig. 4B, as) and the head midline ectoderm (Fig. 4B, he). During stages 6 to 7, the stripe of CG13653 expression widened and became more irregular between the cephalic and the posterior furrows due to the formation of the anterior and posterior transverse furrows (Fig. 4D and F, arrowheads). The expression of CG13653 markedly decreases at later stages of development. Thus, during stage 8 a faint staining was detected in some cells of the amnioserosa and in the head midline ectoderm (Fig. 4G, as and he) to finally became restricted to the procephalic lobe (Fig. 4H, arrowhead). Thus expression of CG13653 fade away at the beginning of germ band extension (stage 8), and not further expression of this gene is detected at later stages of embryogenesis. The transient expression pattern of CG13653 differs from that of the *u-shape* group of Dpp target genes (Frank and Rushlow, 1996), which are expressed throughout amnioserosa formation. Nevertheless, during the restricted period of time that CG13653 is detected in the early embryos, the expression pattern of its mRNA co-localizes with pMad protein in dorsal embryonic regions (Fig. 4C and E), indicating that the temporal and spatial expression pattern of CG13653 was closely correlated with development stages and embryonic regions of active Dpp signaling.

To further analyse the regulation of CG13653 expression, we searched for an enhancer that mediates the expression of CG13653 in the early embryo. Using a bioinformatics approach described in Section 2, we predicted the presence of five clusters of Mad-binding motifs within a 614-bp segment of the 5′-upstream region of CG13653 (clusters M1 to M5). This sequence was contained in a fragment of 1.8 kb isolated from the CG13653 intergenic region, which showed *in vivo* enhancer activity as reported in http://enhancers.starklab.org/ (id: VT47178, Kvon et al., 2014). Interestingly, the pattern of expression of VT47178 recapitulates the *in vivo* expression of CG13653, suggesting that the enhancer of the gene CG13653 is buried within the VT47178 fragment. A closer inspection of a multispecies sequence alignment among *Drosophila* species revealed that predicted Mad-binding motifs were preferentially located in two conserved regions near the transcriptional start site of CG13653 gene. (Supplementary Fig. S2). In order to identify an enhancer that can confer temporally and spatially specific expression of CG13653 in the dorsal ectoderm, three PCR fragments corresponding to conserved segments within the 5`-upstream region of CG13653 were cloned in the pPelican vector and then subjected to *in vivo* testing (Fig. 5). Initially, a fragment containing 808-bp, spanning nucleotides −781 to +27 relative to transcription start site of CG13653, was able to drive *lacZ* expression in a CG13653-like dorsal expression pattern (Fig. 5A). To examine whether the 808-bp enhancer was a Dpp-responsive element, the expression pattern of this reporter construct was examined in a *dpp* null background. In a dpp^{H46} mutant embryo carrying the 808-bp construct, *lacZ* reporter gene expression was abolished (compare Fig. 5A and B). To further define the CG13653 enhancer, two smaller constructs were tested (Fig. 5C and D). Of these, only a fragment of 402-bp (spanning nucleotides −375 to +27) was able to drive a *lacZ* pattern similar to the endogenous CG13653 pattern at stage 5 and stage 7 (Fig. 5D and E). Expression of *lacZ* gene driven by the 402-bp enhancer was not detected beyond the stage 8 of embryogenesis, thus our results indicate that a 402-bp fragment directed expression and mediated responsiveness to Dpp signaling pathway in embryo domains and developmental stages that were comparable

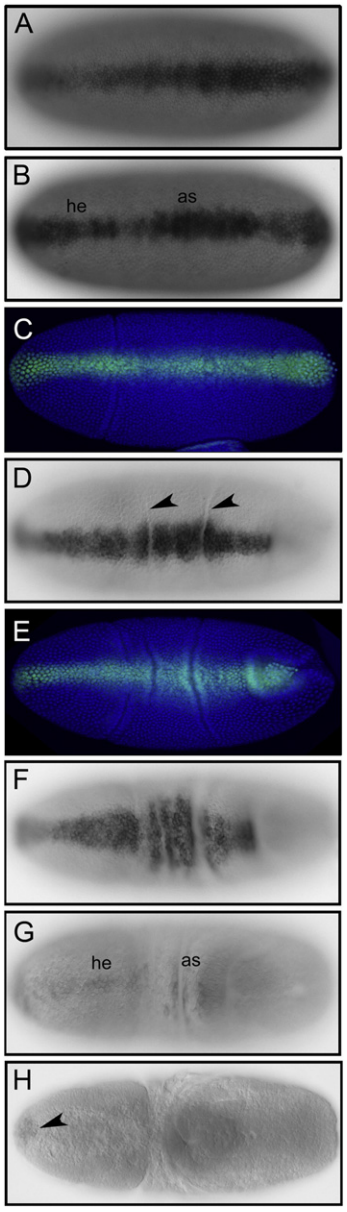

Fig. 4. Expression of CG13653 during embryogenesis. Representative images of whole mount *in situ* hybridizations showing the distribution of CG13653 mRNA in embryos at stage 5 (A), stage 6 (B), stage 7 (D and F), stage 8 (G) and stage 9 (H). Embryos of stage 6 (C) and 7 (E) were stained with an anti-phospho-Smad antibody (green) and ToPro (blue). Amnioserosa (as), head ectoderm (he), arrowheads indicate dorsal transverse furrows. Embryos are oriented with the anterior region to the left, all images are dorsal views.

with the endogenous gene. Then, we induced mutations in the predicted clusters of Mad binding sites in the 402-bp-*lacZ* construct (Fig. 5G). Embryos carrying mutations in clusters M3, M4 and M5 showed a drastic reduction of *lacZ* expression and only few cells remained faintly stained (Fig. 5F). Taken together, these results indicate that the activity of the 402-bp enhancer, and by extrapolation CG13653 expression, in the presumptive amnioserosa and dorsal head regions is under the regulation of Dpp signaling pathway. Within this regulatory region three clusters of Mad binding sites (M3, M4 and M5) are required for Dpp-dependent transcriptional activation of CG13653.

To better describe the response of CG13653 to Dpp, we examined its expression in a sog^{S6} mutant background. Sog is required to generate peak Dpp activity in the embryo dorsal midline (Ashe and Levine, 1999; Podos and Ferguson, 1999). Therefore in the sog^{S6} mutant

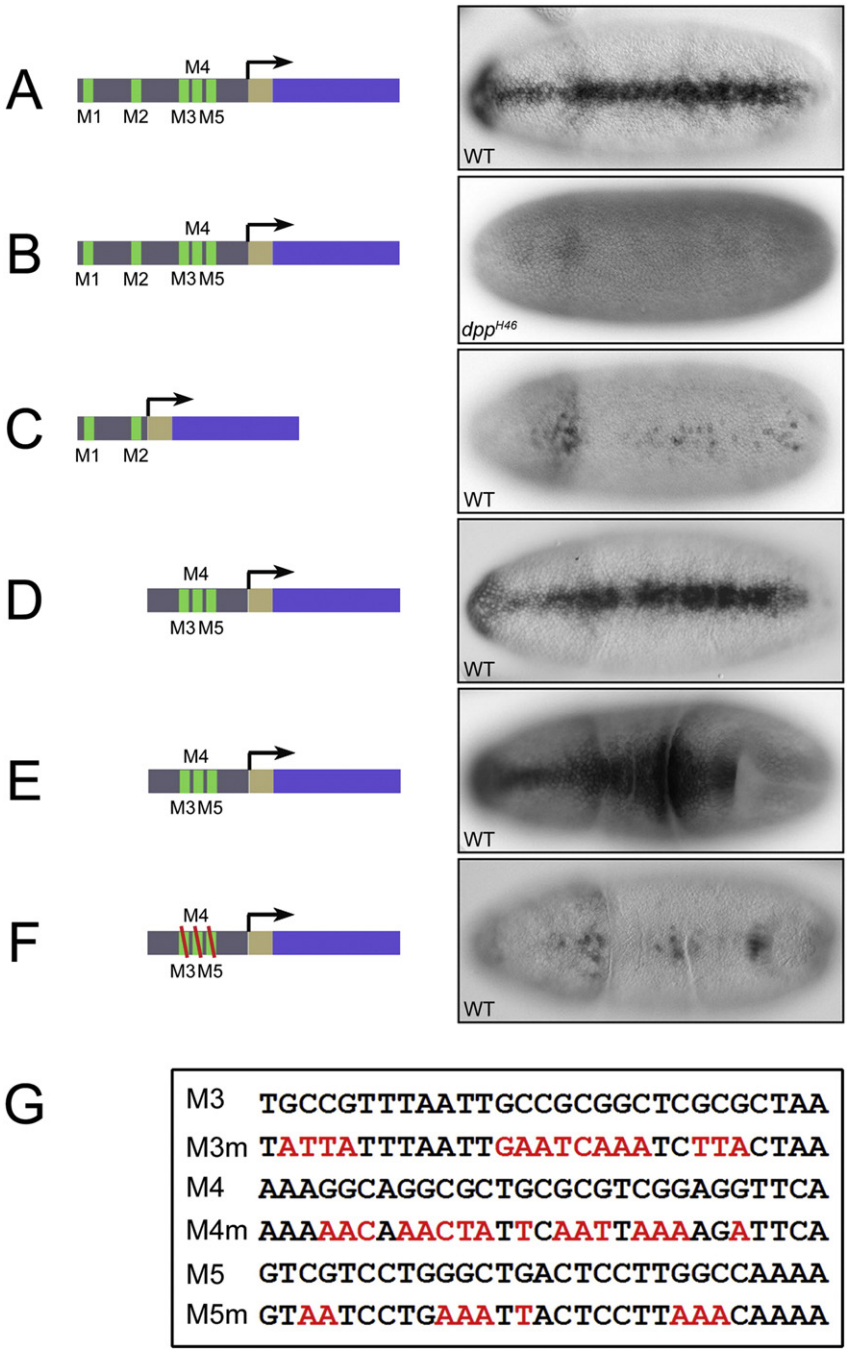

Fig. 5. A 402-bp enhancer drives CG13653 expression. (A) Transgenic embryos of stage 6 carrying the 808-bp-*lacZ* construct were *in situ* hybridized with a *lacZ* probe. (B) Expression of *lacZ* driven by the 808-bp enhancer was undetectable in dpp^{H46} embryos. (C) A 392-bp fragment (spanning nucleotides −389 to −781) drove a weak expression of *lacZ* in small spots. (D) Transgenic embryos of stage 5 or (E) stage 7 carrying the 404-bp-lacZ construct express *lacZ* in pattern highly similar to that of endogenous gene. (F) In an embryo carrying mutations in the clusters M3, M4 and M5 of Mad-binding sites (denoted with a red line), *lacZ* expression is severely reduced. (G) Wild type sequences of the three cluster of Mad binding sites (M3, M4 and M5) and mutations highlighted in red (M3m, M4m and M5m). Genetic backgrounds of transgenic embryos are indicated at the bottom of the panels. Embryos are oriented with the anterior region to the left. All images are dorsal views.

embryos, signaling in the dorsal-most cells decreases and a broad dorsal region of pMad is produced (Dorfman and Shilo, 2001). We observed that the expression of CG13653 was almost completely abolished in the sog^{S6} mutant embryos (Fig. 6A), indicating that proper expression of CG13653 requires peak level of pMad signaling. This observation agrees well with the expression of CG13653 in a narrow dorsal domain that coincides with high pMad levels (Fig. 4). We also examined the effects of mutating *brinker* (*brk*), which encodes a transcriptional repressor that downregulates most Dpp target genes in cells where Dpp pathway is inactive (Jaźwińska et al., 1999). Under this experimental condition we observed that expression of CG13653 was unaffected (Fig. 6B). Thus, the regulation of CG13653 expression seems to be similar to that described for the Dpp target gene, *Ance*, which like CG13653 is expressed at the dorsal-most cells of the embryo and is directly activated by pMad (Xu et al., 2005). In the case of *Ance*, Zen and Mad bind to adjacent sites in the enhancer of the gene, and their interaction is required to activate proper expression of *Ance* in the dorsal-most cells of the embryo. Even though, the identification of functional binding sites for Zen in the CG13653 enhancer is a necessary step to demonstrate that an analogous mechanism is acting to regulate the expression of CG13653, our results

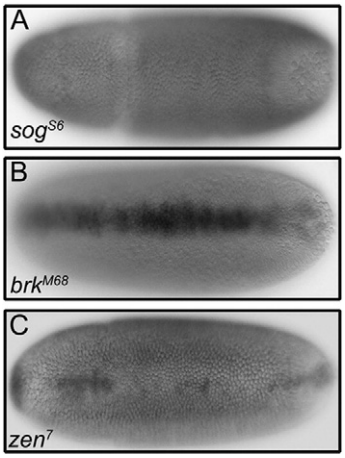

Fig. 6. Expression of CG13653 in mutant backgrounds. Dorsal views of stage 6 embryos with anterior to the left. Mutant sog^{S6} (A), brk^{M68} (B) or zen^{7} (C) embryos were hybridized with a CG13653 probe.

indicate that the activity of Zen is necessary for normal levels of CG13653 expression, because in *zen* mutant embryos only a patchy expression of CG13653 was detected along the dorsal midline (Fig. 4, J). These observations suggest that the expression of CG13653 requires the combined activities of Dpp and Zen.

Taken together, our results indicate that CG13653 is a new component of the gene network activated by Dpp signaling pathway. As was mentioned, CG13653 lacks orthologs in the genomes of mosquitoes and also in the genome of *M. domestica*, a more closely related species, suggesting that CG13653 is a lineage-specific gene. Therefore, we propose that CG13653 might represent an innovation of higher Diptera that was recently incorporated into Dpp signaling network and provide evidences that the activation of CG13653 at early stages of development depends on Dpp signaling pathway and requires peak levels of pMad activity. A future challenge will be to understand which is the role of CG13653 in the early *Drosophila* embryo.

4. Conclusions

In this work we identified a group of genes up-regulated in response to Dpp that were significantly enriched in the dorsal domains of *D. melanogaster* embryos, the amnioserosa and the dorsal ectoderm. Among these genes we found the entire set of genes known to be activated early by Dpp during dorsal ectoderm patterning and a number of genes not previously linked to the Dpp signaling pathway. The expression changes of these genes were validated by quantitative real-time PCR providing an entry point for the investigation of new targets of Dpp regulation in the early embryo. In addition, we characterized a new target gene of the Dpp pathway, CG13653, which encodes a putative secreted protein that lacks orthologs outside of the Drosophilidae family. The expression of CG13653 is temporally restricted to early stages of development, when the dorsal ectoderm patterning takes place, and spatially restricted to dorsal embryo domains with peak level of Dpp/Scw signaling. Further studies should be performed to place CG13653 actions within known mechanisms of regulation of Dpp pathway.

Supplementary data to this article can be found online at http://dx.doi.org/10.1016/j.gene.2016.07.015.

Acknowledgements

This work was supported by FONDECYT 1120254 to VC FONDECYT 11130231 to CH and FONDAP 15090007 to VC, CH and MG. CD was supported by postdoctoral FONDECYT project No. 3140007. We thanks the Bloomington Drosophila Stock Center for providing stocks used in this study. We acknowledge the Confocal Unit at INTA-University of Chile (FondEquip EQM120153).

References

Arora, K., Levine, M.S., O'Connor, M.B., 1994. The screw gene encodes a ubiquitously expressed member of the TGF-beta family required for specification of dorsal cell fates in the *Drosophila* embryo. Genes Dev. 8 (21), 2588–2601.
Ashe, H.L., Levine, M., 1999. Local inhibition and long-range enhancement of Dpp signal transduction by Sog. Nature 398 (6726), 427–431.
Ashe, H.L., Mannervik, M., Levine, M., 2000. Dpp signaling thresholds in the dorsal ectoderm of the *Drosophila* embryo. 127 (15), 3305–3312.
Attrill, H., Falls, K., Goodman, J.L., Millburn, G.H., Antonazzo, G., Rey, A.J., Marygold, S.J., FlyBase, C., 2015. FlyBase: establishing a gene group resource for *Drosophila melanogaster*. Nucleic Acids Res.
Barolo, S., Carver, L., Posakony, J., 2000. GFP and beta-galactosidase transformation vectors for promoter/enhancer analysis in *Drosophila*. Biotechniques 29 (4) (726, 728, 730, 732).
Bellen, H.J., Levis, R.W., Liao, G., He, Y., Carlson, J.W., Tsang, G., Evans-Holm, M., Hiesinger, P.R., Schulze, K.L., Rubin, G.M., Hoskins, R.A., Spradling, A.C., 2004. The BDGP gene disruption project: single transposon insertions associated with 40% of *Drosophila* genes. Genetics 167 (2), 761–781.
Benjamini, Y., Hochberg, Y., 1995. Controlling the false discovery rate: a practical and powerful approach to multiple testing. J. R. Stat. Soc. 57 (1), 289–300.
Brudno, M., Do, C.B., Cooper, G.M., Kim, M.F., Davydov, E., Program, N.C.S., Green, E.D., Sidow, A., Batzoglou, S., 2003. LAGAN and multi-LAGAN: efficient tools for large-scale multiple alignment of genomic DNA. Genome Res. 13, 721–731.
Campos-Ortega, J.A., Hartenstein, V., 1985. The Embryonic Development of *Drosophila melanogaster*. Springer, Berlin.
Chang, T., Mazotta, J., Dumstrei, K., Dumitrescu, A., Hartenstein, V., 2001. Dpp and Hh signaling in the *Drosophila* embryonic eye field. Development 128 (23), 4691–4704.
Chen, D., McKearin, D., 2003. Dpp signaling silences bam transcription directly to establish asymmetric divisions of germline stem cells. Curr. Biol. 13 (20), 1786–1791.
Dequier, E., Souid, S., Pal, M., Maroy, P., Lepesant, J.A., Yanicostas, C., 2001. Top-DER- and Dpp-dependent requirements for the *Drosophila* fos/kayak gene in follicular epithelium morphogenesis. Mech. Dev. 106 (1–2), 47–60.
Dorfman, R., Shilo, B.Z., 2001. Biphasic activation of the BMP pathway patterns the *Drosophila* embryonic dorsal region. Development 128 (6), 965–972.
Edgar, R.C., 2004. MUSCLE: multiple sequence alignment with high accuracy and high throughput. Nucleic Acids Res. 32 (5), 1792–1797.
Frank, L.H., Rushlow, C., 1996. A group of genes required for maintenance of the amnioserosa tissue in *Drosophila*. Development 122 (5), 1343–1352.
Frazer, K.A., Pachter, L., Poliakov, A., Rubin, E.M., Dubchak, I., 2004. VISTA: computational tools for comparative genomics. Nucleic Acids Res. 32, W273–W279.
Gavin-Smyth, J., Wang, Y.C., Butler, I., Ferguson, E.L., 2013. A genetic network conferring canalization to a bistable patterning system in *Drosophila*. Curr. Biol. 23 (22), 2296–2302.
Ghanim, M., White, K., 2006. Genotyping method to screen individual *Drosophila* embryos prior to RNA extraction. Biotechniques 41 (4) (414, 416, 418).
Hamaguchi, T., Yabe, S., Uchiyama, H., Murakami, R., 2004. Drosophila Tbx6-related gene, Dorsocross, mediates high levels of Dpp and Scw signal required for the development of amnioserosa and wing disc primordium. Dev. Biol. 265 (2), 355–368.
Hammonds, A.S., Bristow, C.A., Fisher, W.W., Weiszmann, R., Wu, S., Hartenstein, V., Kellis, M., Yu, B., Frise, E., Celniker, S.E., 2013. Spatial expression of transcription factors in *Drosophila* embryonic organ development. Genome Biol. 14 (12), R140.
Hertz, G.Z., Stormo, G.D., 1999. Identifying DNA and protein patterns with statistically significant alignments of multiple sequences. Bioinformatics 15 (7–8), 563–577.
Hodar, C., Zuniga, A., Pulgar, R., Travisany, D., Chacon, C., Pino, M., Maass, A., Cambiazo, V., 2014. Comparative gene expression analysis of Dtg, a novel target gene of Dpp signaling pathway in the early *Drosophila melanogaster* embryo. Gene 535 (2), 210–217.
Jaźwińska, A., Kirov, N., Wieschaus, E., Roth, S., Rushlow, C., 1999. The *Drosophila* gene brinker reveals a novel mechanism of Dpp target gene regulation. Cell 96 (4), 563–573.
Kim, J., Johnson, K., Chen, H.J., Carroll, S., Laughon, A., 1997. Drosophila Mad binds to DNA and directly mediates activation of vestigial by decapentaplegic. Nature 388 (6639), 304–308.
Kvon, E.Z., Kazmar, T., Stampfel, G., Yanez-Cuna, J.O., Pagani, M., Schernhuber, K., Dickson, B.J., Stark, A., 2014. Genome-scale functional characterization of *Drosophila* developmental enhancers in vivo. Nature 512 (7512), 91–95.
Liang, H.-L., Xu, M., Chuang, Y.-C., Rushlow, C., 2012. Response to the BMP gradient requires highly combinatorial inputs from multiple patterning systems in the *Drosophila* embryo. Development 139 (11), 1956–1964.
Lin, M.-C., Park, J., Kirov, N., Rushlow, C., 2006. Threshold response of C15 to the Dpp gradient in *Drosophila* is established by the cumulative effect of Smad and Zen activators and negative cues. Development 133 (24), 4805–4813.
Liu, T.-H., Li, L., Vaessin, H., 2002. Transcription of the *Drosophila* CKI gene dacapo is regulated by a modular array of cis-regulatory sequences. Mech. Dev. 112 (1–2), 25–36.
Lyne, R., Smith, R., Rutherford, K., Wakeling, M., Varley, A., Guillier, F., Janssens, H., Ji, W., McLaren, P., North, P., Rana, D., Riley, T., Sullivan, J., Watkins, X., Woodbridge, M., Lilley, K., Russell, S., Ashburner, M., Mizuguchi, K., Micklem, G., 2007. FlyMine: an integrated database for *Drosophila* and *Anopheles* genomics. Genome Biol. 8 (7), R129.
Matsuda, S., Harmansa, S., Affolter, M., 2016. BMP morphogen gradients in flies. Growth Factor Rev. 27, 119–127.
Parker, L., Stathakis, D.G., Arora, K., 2004. Regulation of BMP and activin signaling in *Drosophila*. Prog. Mol. Subcell. Biol. 34, 73–101.

Pfaffl, M.W., 2001. A new mathematical model for relative quantification in real-time RT-PCR. Nucleic Acids Res. 29 (9), e45.
Podos, S.D., Ferguson, E.L., 1999. Morphogen gradients: new insights from DPP. Trends Genet. 15 (10), 396–402.
Rafiqi, A.M., Lemke, S., Ferguson, S., Stauber, M., Schmidt-Ott, U., 2008. Evolutionary origin of the amnioserosa in cyclorrhaphan flies correlates with spatial and temporal expression changes of zen. Proc. Natl. Acad. Sci. U. S. A. 105 (1), 234–239.
Raftery, L.A., Sutherland, D.J., 2003. Gradients and thresholds: BMP response gradients unveiled in *Drosophila* embryos. Trends Genet. 19 (12), 701–708.
Reim, I., Lee, H.-H., Frasch, M., 2003. The T-box-encoding Dorsocross genes function in amnioserosa development and the patterning of the dorsolateral germ band downstream of Dpp. Development 130 (14), 3187–3204.
Ritchie, M.E., Silver, J., Oshlack, A., Holmes, M., Diyagama, D., Holloway, A., Smyth, G.K., 2007. A comparison of background correction methods for two-colour microarrays. Bioinformatics 23 (20), 2700–2707.
Rusch, J., Levine, M., 1997. Regulation of a dpp target gene in the *Drosophila* embryo. Development 124 (2), 303–311.
Rushlow, C., Arora, K., 1990. Dorsal ventral polarity and pattern formation in the *Drosophila* embryo. Semin. Cell Biol. 1 (3), 137–149.
Rushlow, C., Colosimo, P.F., Lin, M.C., Xu, M., Kirov, N., 2001. Transcriptional regulation of the *Drosophila* gene zen by competing Smad and Brinker inputs. Genes Dev. 15 (3), 340–351.
Saunders, A., Core, L.J., Sutcliffe, C., Lis, J.T., Ashe, H.L., 2013. Extensive polymerase pausing during *Drosophila* axis patterning enables high-level and pliable transcription. Genes Dev. 27 (10), 1146–1158.
Schmidt-Ott, U., Rafiqi, A.M., Lemke, S., 2010. Hox3/zen and the evolution of extraembryonic epithelia in insects. Adv. Exp. Med. Biol. 689, 133–144.
Scuderi, A., Simin, K., Kazuko, S.G., Metherall, J.E., Letsou, A., 2006. scylla and charybde, homologues of the human apoptotic gene RTP801, are required for head involution in *Drosophila*. Dev. Biol. 291 (1), 110–122.
Smyth, G.K., 2004. Linear models and empirical Bayes methods for assessing differential expression in microarray experiments. Stat. Appl. Genet. Mol. Biol. 3, 3.
Smyth, G.K., Speed, T., 2003. Normalization of cDNA microarray data. Methods 31 (4), 265–273.
Talke, I.N., Hanikenne, M., Kramer, U., 2006. Zinc-dependent global transcriptional control, transcriptional deregulation, and higher gene copy number for genes in metal homeostasis of the hyperaccumulator *Arabidopsis halleri*. Plant Physiol. 142 (1), 148–167.
ten Dijke, P., Miyazono, K., Heldin, C.H., 2000. Signaling inputs converge on nuclear effectors in TGF-beta signaling. Trends Biochem. Sci. 25 (2), 64–70.
Thuringer, F., Cohen, S.M., Bienz, M., 1993. Dissection of an indirect autoregulatory response of a homeotic *Drosophila* gene. EMBO J. 12 (6), 2419–2430.
Tomancak, P., Beaton, A., Weiszmann, R., Kwan, E., Shu, S., Lewis, S.E., Richards, S., Ashburner, M., Hartenstein, V., Celniker, S.E., Rubin, G.M., 2002. Systematic determination of patterns of gene expression during *Drosophila* embryogenesis. Genome Biol. 3 (12) (RESEARCH0088).
Tomancak, P., Berman, B.P., Beaton, A., Weiszmann, R., Kwan, E., Hartenstein, V., Celniker, S.E., Rubin, G.M., 2007. Global analysis of patterns of gene expression during *Drosophila* embryogenesis. Genome Biol. 8 (7), R145.
Wang, X., Ghosh, S., Guo, S.W., 2001. Quantitative quality control in microarray image processing and data acquisition. Nucleic Acids Res. 29 (15), E75.
Wang, X., Harris, R.E., Bayston, L.J., Ashe, H.L., 2008. Type IV collagens regulate BMP signalling in *Drosophila*. Nature 455 (7209), 72–77.
Waterhouse, R.M., Zdobnov, E.M., Tegenfeldt, F., Li, J., Kriventseva, E.V., 2011. OrthoDB: the hierarchical catalog of eukaryotic orthologs in 2011. Nucleic Acids Res. 39 (Database issue), D283–D288.
Weiss, A., Charbonnier, E., Ellertsdóttir, E., Tsirigos, A., Wolf, C., Schuh, R., Pyrowolakis, G., Affolter, M., 2010. A conserved activation element in BMP signaling during *Drosophila* development. Nat. Struct. Mol. Biol. 17 (1), 69–76.
Wharton, K., Ray, R., Gelbart, W., 1993. An activity gradient of decapentaplegic is necessary for the specification of dorsal pattern elements in the *Drosophila* embryo. Development 117 (2), 807–822.
Wharton, S.J., Basu, S.P., Ashe, H.L., 2004. Smad affinity can direct distinct readouts of the embryonic extracellular Dpp gradient in *Drosophila*. Curr. Biol. 14 (17), 1550–1558.
Wolpert, L., 1996. One hundred years of positional information. Trends Genet. 12 (9), 359–364.
Xu, X., Yin, Z., Hudson, J.B., Ferguson, E.L., Frasch, M., 1998. Smad proteins act in combination with synergistic and antagonistic regulators to target Dpp responses to the *Drosophila* mesoderm. Genes Dev. 12 (15), 2354–2370.
Xu, M., Kirov, N., Rushlow, C., 2005. Peak levels of BMP in the *Drosophila* embryo control target genes by a feed-forward mechanism. Development 132 (7), 1637–1647.
Yip, M.L., Lamka, M.L., Lipshitz, H.D., 1997. Control of germ-band retraction in *Drosophila* by the zinc-finger protein HINDSIGHT. Development 124 (11), 2129–2141.
Zúñiga, A., Hödar, C., Hanna, P., Ibáñez, F., Moreno, P., Pulgar, R., Pastenes, L., González, M., Cambiazo, V., 2009. Genes encoding novel secreted and transmembrane proteins are temporally and spatially regulated during *Drosophila melanogaster* embryogenesis. BMC Biol. 7, 61.